Structure-property relations of nanophase-separated poly(pentyl methacrylate-*b*-methyl methacrylate) diblock copolymers

Das Projekt wurde im Rahmen des EU NoE NANOFUN-POLY zusammen mit Partnern aus Italien, Spanien und Griechenland durchgeführt. Es zielt auf die Entwicklung von nanostrukturierten Oberflächen basierend auf wohl definierten Poly(pentylmethacrylat-b-methylmethacrylat)-Diblockcopolymeren (PPMA/PMMA), die mittels anionischer Polymerisation synthetisiert wurden. Durch zusätzliches Einbringen von Nanoobjekten und Einstellen der Wechselwirkung zwischen Polymer und Nanoobjekt, zum Beispiel durch gezieltes Erzeugen von Funktionalitäten und Erweiterung um einen chemisch andersartigen Block, soll die Nanostrukturierung zusätzlich kontrolliert werden. So wurden die Blockcopolymere mit Nanopartikeln oder Schichtsilikaten gemischt bzw. in einem Sol-Gel-Prozess mit Metallalkoxiden eingesetzt. Die Kette der Untersuchungen umfasste die Synthese, Untersuchung der Festkörperstruktur, Untersuchung der Struktur in dünnen Filmen sowie die Bestimmung des makroskopischen Benetzungsverhaltens mit Wasser und Proteinlösungen. Es konnte gezeigt werden, dass PPMA/PMMA-Diblockcopolymere reguläre Nanostrukturen in dünnen Filmen ausbilden können.

Nanostructured materials based on diblock copolymers have gained large interest in the last decades because they offer the opportunity to use the micro-phase separation of diblock copolymers [1-3] (which actually takes place on the nanoscale level) caused by the chemical immiscibility of the blocks to develop materials with nanostructures not only in the bulk but also in thin films or at surfaces [4]. Nanotechnology with block copolymers [5] has therefore become one of the most innovative fields of polymer science providing materials for applications as templates, patterned substrates, 2D photonic crystals, wave guides, and many others. The research project reported here was carried out within the framework of *EU NoE NANOFUN-POLY* (Internal project 4). It was directed to the development of nanostructured surfaces based on the phase separation of poly(pentyl methacrylate-*b*-methyl methacrylate) diblock copolymers (PPMA/PMMA) and their additional interaction with inorganic nanoobjects obtained by different methods. To achieve this goal, the chain of knowledge starting from

(1) controlled synthesis of the block copolymers and their chemical characterization,
(2) introduction of functional groups able to react or interact with inorganic objects,
(3) characterization of the phase separation in solid state (bulk),
(4) characterization of the morphology and phase separation in thin films by a combination of advanced physical methods,
(5) characterization of the surface properties (macroscopic wetting and protein adsorption), and
(6) the alteration of all these properties by incorporation of inorganic nanoobjects

had to be intensively investigated. The PPMA/PMMA diblock copolymer system was chosen for the project because of the fairly high interaction parameter [6] allowing a pronounced phase separation

Keywords
anionic polymerization
diblock copolymers
nanophase separation
nanostructured surfaces
nanoobjects

Bearbeiter
D. Pospiech
D. Jehnichen
S. Ptacek
R. Keska
K. Eckstein
P. Friedel
H. Komber
A. Janke
K. Grundke
M. Sangermano
F. Simon
J. Bunk
F. Näther
B. Voit
M. Stamm

Förderer
Europäische Union, Network of Excellence NANOFUN-POLY
Deutscher Akademischer Austauschdienst (Ikyda Programm)
Humboldt-Stiftung

Kooperation
Prof. R. Bongiovanni,
Prof. M. Sangermano,
Politecnico di Torino, Italy
Dr. S. Funari,
DESY Hamburg, Hasylab
Dr. H. Reinecke,
CSIC, Madrid, Spain
Prof. C. Papadakis,
University of Munich
Prof. F. Pilati,
University of Modena and Reggio Emilia, Italy
Prof. P. Pissis,
National Technical University of Athens, Greece
Prof. C. Tsitsilianis,
FORTH, Patras, Greece

Gastwissenschaftler
S. Kripotou,
National Technical University of Athens, Greece
R. Navarro,
CSIC Madrid, Spain
M. Sangermano, A. Di Gianni,
Politecnico di Torino, Italy
R. Taurino,
University of Modena and Reggio Emilia, Italy

Arbeitsaufenthalte
D. Jehnichen, S. Ptacek, P. Friedel,
DESY Hamburg, Hasylab
S. Ptacek, D. Pospiech,
D. Jehnichen, National Technical University of Athens, Greece

in the block copolymers while maintaining a certain level of chemical similarity. Based on the knowledge of the phase separation behavior of PPMA/PMMA diblock copolymers in bulk as reported previously [7], PPMA/PMMA diblock copolymers with preferably lamellar and cylindrical structure were synthesized and subsequently tagged with functional groups.

Synthesis of PPMA/PMMA diblock copolymers

The synthesis of PPMA/PMMA diblock copolymers used in the subsequent working steps was performed by sequential living anionic polymerization of pentyl methacrylate and methyl methacrylate in tetrahydrofuran (THF) at -78 °C, based on a procedure given by Scherble et al. [6], and reported previously by our group [7].

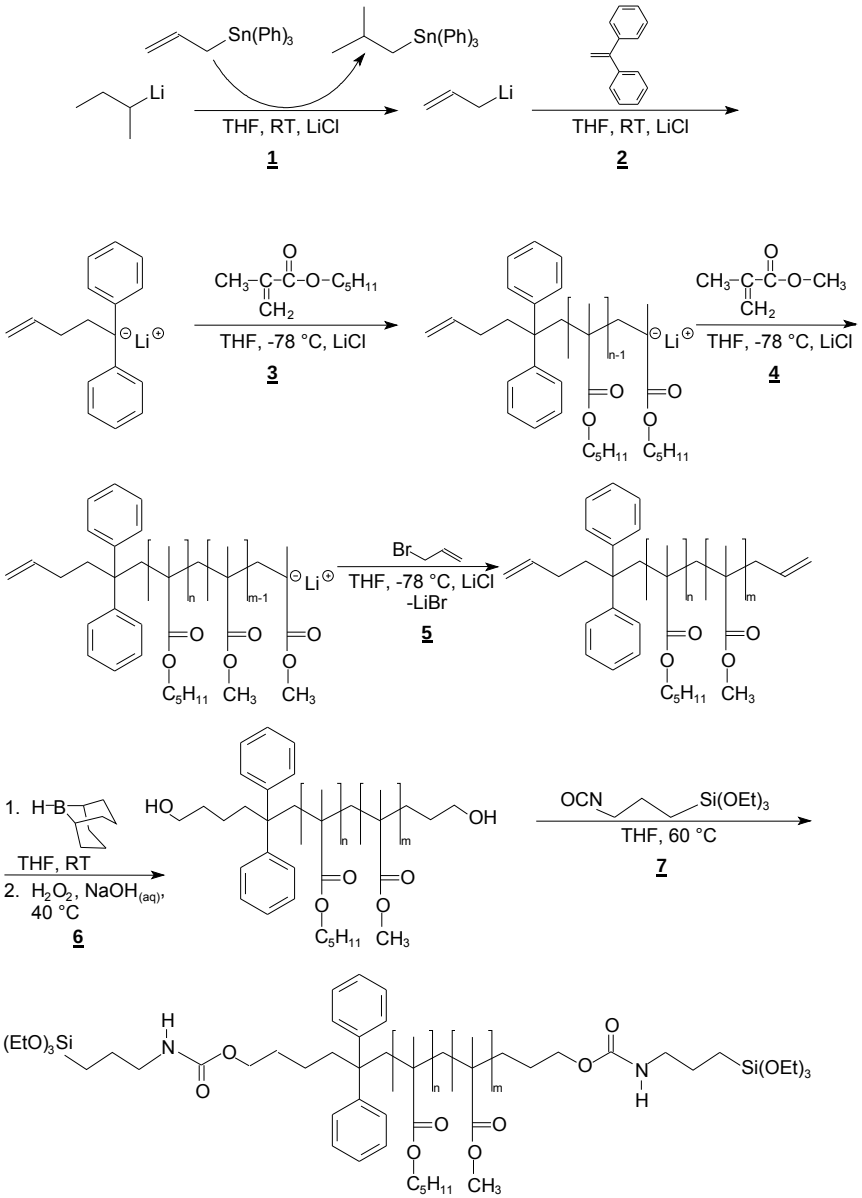

Fig. 1:
Reaction scheme for the synthesis of functionalized PPMA/PMMA diblock copolymers
1 *and* ***2****: synthesis of allyl-terminated initiator;*
3*: synthesis of poly(pentyl methacrylate) block;*
4*: synthesis of poly(methyl methacrylate) block;*
5*: end-capping with allyl bromide;*
6*: conversion of allyl groups into OH-groups by hydroboration;*
7*: reaction of OH-end groups with 3-isocyanatopropyl triethoxy silane to triethoxysilane-terminated BCP*

The normal procedure using the product of *sec*-butyl lithium (*sec*-BuLi) and 1,1-diphenyl ethylene (DPE) as initiator which results in non-functionalized block copolymers (BCP) after quenching with methanol [8] had to be modified in order to obtain BCP with functional groups. The reaction scheme based on [9] chosen among several possibilities described in the literature [e.g. 10] is given in Fig. 1.

The conventional procedure with *sec*-BuLi/DPE initiator end-capped with allyl bromide [10] gave mono-allyl-functionalized BCP, while the synthesis using 1,1-diphenyl pent-4-enyl-lithium initiator according to steps **1**-**5** in Fig. 1 yielded di-allyl-functionalized BCP. The allyl groups were converted via hydroboration into OH-groups (step **6**) and, finally, into triethoxysilane end groups (step **7**) in order to provide BCP with functional groups useful in sol-gel processes and in nanocomposites. The successful conversion from allyl into OH-functionalized groups could not directly be detected by ^{1}H-NMR spectroscopy and had to be proven by the reaction of presumably OH-terminated BCPs with trichloroacetyl isocyanate. One example is illustrated in Fig. 2.

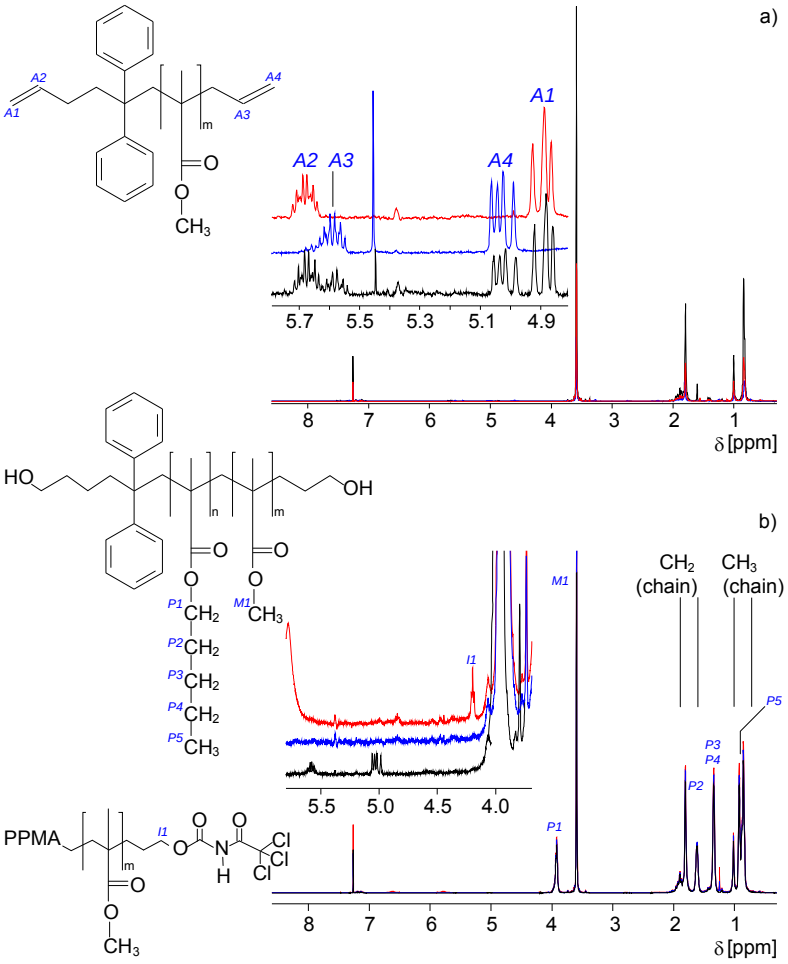

Fig. 2:
^{1}H NMR spectra of
a) allyl-functionalized PMMA (—— AMA44; —— MA49; —— AM33) and
b) OH-terminated PPMA/PMMA block copolymer PM-OH (—— PMA19; —— PMOH19; —— PMOH19 + isocyanate)

The polydispersities PDI (M_w/M_n) of the block copolymers with different molar masses and compositions (Tab. 1) were low as it could be expected from anionic polymerization. Functionalization by the procedures described above did not increase the PDI.
PPMA/PMMA block copolymers could also be obtained by applying controlled radical polymerization (atom transfer radical polymerization, ATRP). Even though the resulting products had lower molar masses (up to 50000 g·mol^{-1}) and a higher PDI (1.2 to 1.3) than BCP prepared by anionic polymerization, it could be proven by T-SAXS that also these materials were able to form regular nanostructures [11].

Sample	Composition PPMA/PMMA [mol / mol]	$M_{w,SEC}$ [g·mol^{-1}]	PDI [$M_{w,SEC}/M_{n,SEC}$]	d[1)] [nm]	Bulk morphology
Non-functionalized:					
PM01	74 / 26	185800	1.06	58	lamellar
PM03	67 / 33	84300	1.04	41	cylindrical
PM04	67 / 33	65200	1.04	35	cylindrical
PM05	68 / 32	18100	1.03	14	weak[2]
PM20	48 / 52	26200	1.03	22	lamellar
PM16	40 / 60	143000	1.12	25	lamellar
AR77	37 / 63	113400	1.10	45	lamellar
AR78	37 / 63	77300	1.07	46	lamellar
Mono-functionalized:					
PMA21	39 / 61	30300	1.04	25	lamellar
PMOH21	39 / 61	30800	1.03	26	lamellar
PMA19	39 / 61	28500	1.04	24	lamellar
PMOH19	39 / 61	27400	1.04	24	lamellar
APM26	43 / 57	25300	1.08	22	lamellar
HOPM26	43 / 57	25200	1.05	20	lamellar
AM33	0 / 100	8700	1.05	-	-
MA49	0 / 100	6050	1.05	-	-
Di-functionalized:					
APMA28	38 / 62	27400	1.09	24	lamellar
HOPMOH28	38 / 62	26500	1.07	23	lamellar
AMA44	0 / 100	21600	1.04	-	-

Tab. 1:
Composition, molar masses and bulk morphology of selected PPMA/PMMA diblock copolymers.
[1)] Periodicity d found in small-angle X-ray scattering (SAXS) of bulk samples annealed in vacuum at 140 °C for 4 h
[2)] Sample with a non-pronounced morphology

Phase separation in solid state

The phase separation behavior was estimated using the BCP phase diagram obtained by mean field calculation based on an approach published by Leibler [12] and Benoit et al. [13]. The low PDI of the BCP allowed the use of spinodals for mono-disperse BCPs, without further regarding the polydispersity which shifts the spinodals to higher values [14]. The BCP synthesized were plotted in the phase diagram (Fig. 3, containing only the samples discussed in this report) after calculation of χ-parameter and number of repeating units N of the BCP (calculation example in [15]). The experimentally observed phase behavior was compared to the predicted one and a good correlation was found (see also [7]). Most of the BCPs synthesized were phase separated and did not show an order-disorder transition in temperature-dependent small-angle X-ray scattering (T-SAXS, performed at DESY Hamburg, HASYLAB, beamline A2), thus reflecting the high tendency of phase separation despite the fact that both blocks are chemically rather similar. Only BCP with total molar masses below about 10000 g·mol^{-1} and asymmetric composition were homogeneous and non-phase separated (e.g., sample PM05 marked in Fig. 3 with an arrow). The phase diagram does not reflect the morphology of the BCP, which had to be experimentally examined by SAXS and atomic force microscopy (AFM, morphology of inner surfaces of cut bulk samples obtained by annealing and compression of powder). Most of the samples in the phase diagram formed a well-pronounced lamellar structure. Only samples in the compositional region of PPMA/PMMA 70-66 / 30-24 mol/mol showed cylindrical structures or mixed lamellae/cylinders, as confirmed by both methods. The SAXS periodicities d corresponded to the total molar mass of the BCP. The introduction of functionalities did not significantly change neither the type of morphology nor the d-value (Tab. 1). However it can be observed that BCP with lower total molar masses (about 20000 g·mol^{-1} and lower) do not form a pronounced morphology.

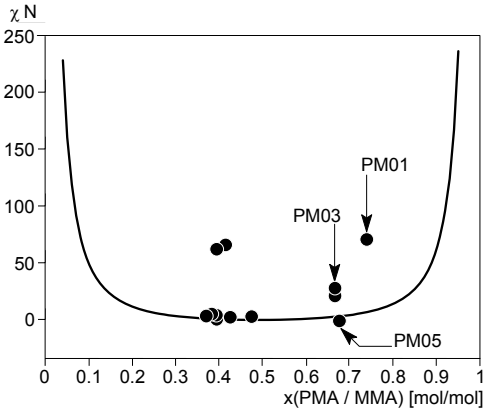

Fig. 3:
Mean field phase diagram of PPMA/PMMA diblock copolymers, mono-disperse case (x = molar fraction)

Figures 4 and 5 show exemplarily the SAXS curves of a lamellar and a cylindrical BCP with temperature (no order-disorder transition (ODT), improvement of structure with temperature) and Fig. 6 illustrates the corresponding bulk morphology images and confirmed the formation of well-ordered lamellae with periodicities in the range of 15 to 55 nm and well-defined temperature dependence [16]. The analysis of glass transition temperatures from DSC by Fox-Flory calculations reflected, however, that the PMMA phase (bright in the AFM image) always contained considerable amounts of PPMA (partial intermixing, despite the well-phase separated morphology) [7]. The wide range of lamellar structures in PPMA/PMMA compared to other types of BCP and the absence of bi-continuous structures may be explained by the chemical similarity of both blocks. End-capping of PPMA/PMMA by allyl groups or OH-groups had only a minor influence on the bulk morphology.

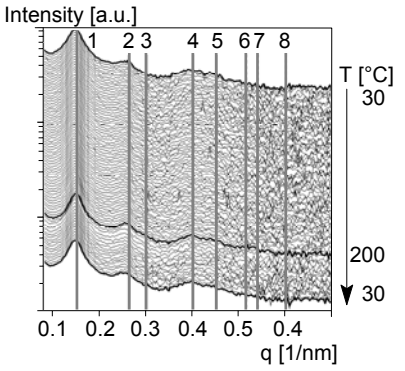

Fig. 4:
Transmission-SAXS curves of the cylindrical BCP PM03 having an hcp unit cell with a_{hex} = 48.4 nm. Assignment:
1 – $d_{(100)}$ = 41.9 nm,
2 – $d_{(110)}$,
3 – $d_{(200)}$,
4 – $d_{(210)}$,
5 – $d_{(300)}$,
6 – $d_{(220)}$,
7 – $d_{(310)}$,
8 – $d_{(400)}$

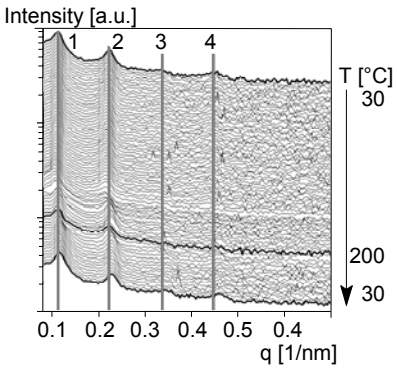

Fig. 5:
Transmission-SAXS curves of the lamellar BCP PM01. Assignment:
1 – 1st order reflection with $d_{(100)}$ = 55.0 nm,
2 – $d_{(200)}$,
3 – $d_{(300)}$,
4 – $d_{(400)}$

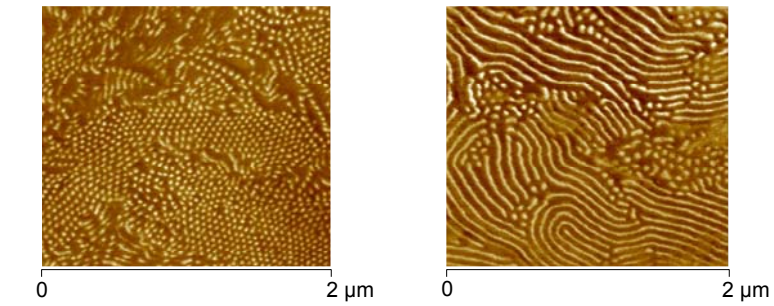

Fig. 6:
AFM phase images of PPMA/PMMA diblock copolymers (cut bulk samples)
Left: PM03 (PPMA/PMMA 67/33 mol/mol)
Right: PMO1(PPMH/PMMA 74/26 mol/mol)

Structure, morphology and wetting properties of thin films

Thin films of diblock copolymers with cylindrical and lamellar bulk morphology on silicon wafer with a polymer film thickness between 25 and 120 nm (measured by ellipsometry) and very low roughness (below 1 nm, measured by AFM) were obtained by dip coating silicon wafers into low concentrated polymer solutions in THF. The morphology was examined by AFM and grazing incidence small angle X-ray scattering (GISAXS, see e.g. [17]) at the DESY Synchrotron. The efforts aimed at laterally demixed morphologies (standing lamellae or cylinders). The morphologies of the resulting thin films depended on the chemical composition of the BCP (as in the bulk) as well as the molar mass.
Figures 7-10 illustrate a few examples (left: AFM phase contrast image; center: schematic morphology derived from GISAXS [18]), (right: GISAXS 2D plot). Very thin films with a thickness in the range or below the bulk periodicity d indeed showed standing cylinders (Fig. 7) or standing lamellae (Fig. 9) where the lamellae are arranged in a wavy structure, but lateral to the surface. Thicker films with thickness higher than d_{bulk} gave lying cylinders (Fig. 8) or lamellae (Fig. 10) arranged parallel to the surface. The periodicities of nanostructures in the thin films were comparable to the periodicities obtained in the bulk samples (cf. Tab. 1).

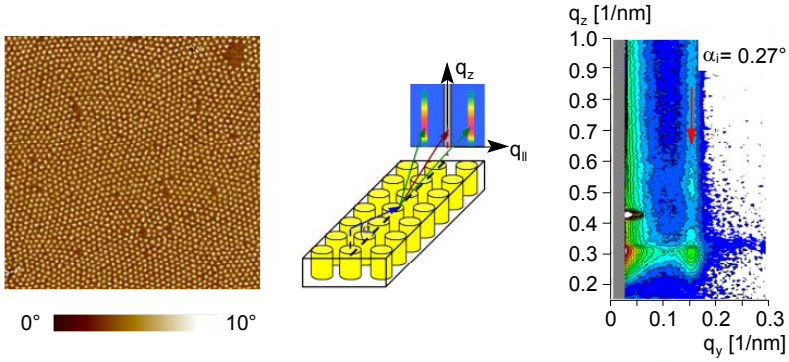

Fig. 7:
BCP PM03
(PPMA/PMMA 67/33 mol/mol)
Thickness: 25 nm
Morphology: standing PMMA cylinders (hcp) normal to the surface

[O]:[C] ratio: 0.236 Lateral repeat distance: 41.1 nm
PPMA/PMMA at the surface: 91/9 mol/mol
Contact angle: 96.0°

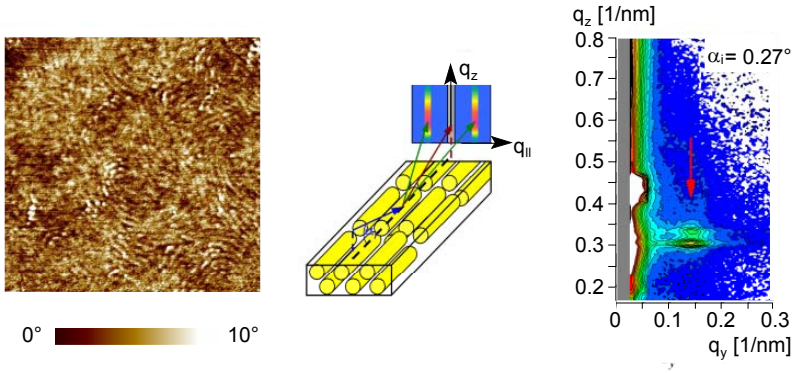

Fig. 8:
BCP PM03
(PPMA/PMMA 67/33 mol/mol)
Thickness: 45 nm
Morphology: short lying PMMA cylinders parallel to the surface

[O]:[C] ratio: 0.227 Lateral repeat distance: 43.9 nm
PPMA/PMMA at the surface: 96/4 mol/mol
Contact angle: 97.5°

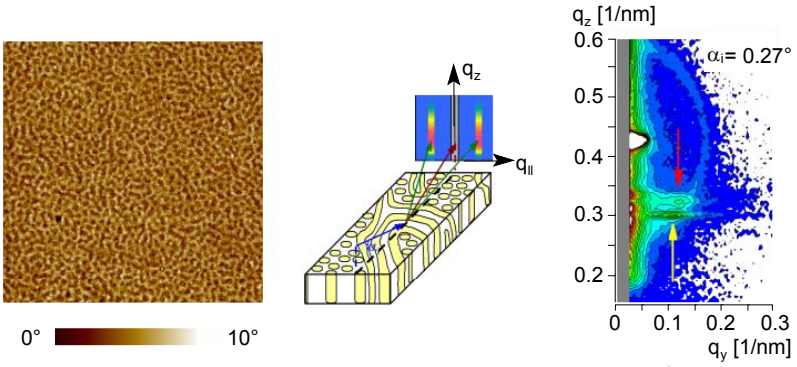

Fig. 9:
BCP PM01
(PPMA/PMMA 74/26 mol/mol)
Thickness: 55 nm
Morphology: Mixture of standing PPMA cylinders and very short lamellae normal to the surface

[O]:[C] ratio: 0.216 Lateral repeat distance: 43.9 nm
PPMA/PMMA at the surface: 100/0 mol/mol
Contact angle: 97.6°

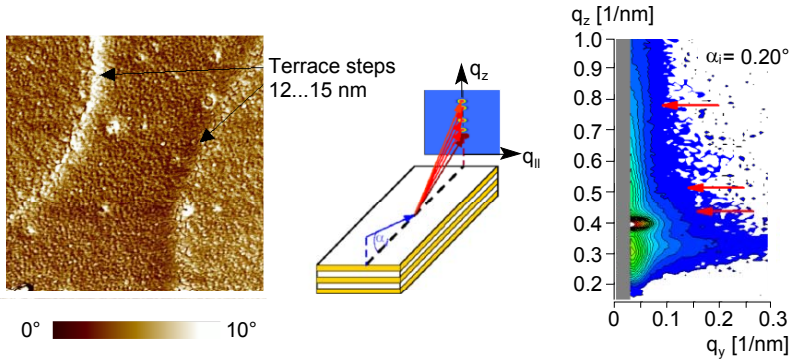

Fig. 10:
BCP AR39
(PPMA/PMMA 39/61 mol/mol)
Thickness: 27 nm
Morphology: lying lamellae parallel to the surface

Contact angle: 91.2° No lateral repeat distance

Figures 7-9 also contain the surface composition determined by XPS (maximum information depth ca. 8 nm), expressed as [O]:[C] ratio, and the advancing water contact angles. Both parameters differed only slightly for almost all block copolymers, independent of composition and total molar mass. Intensive investigation of the macroscopic wetting behavior [19] verified this result.
It had to be concluded that the nanostructured surfaces obtained from PPMA/PMMA block copolymers were in most cases covered by a nanometer thin layer of the PPMA block (which is the low surface free energy block and enriched therefore near the surface), despite the nanostructure detected by AFM stiffness contrast. Thus, the macroscopic wetting behavior of the BCP was very close to PPMA. The low contact angles of PMMA (around 75°) could not be reached even if some PMMA is at the surface because the PMMA phase always contained dissolved PPMA.

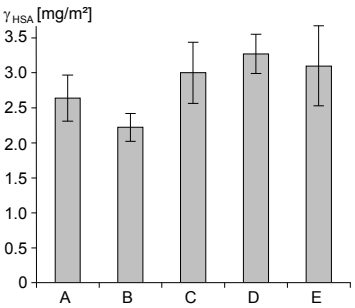

Fig. 11:
Adsorbed amounts of human serum albumin (γ_{HSA}) on thin polymer films after 1 hour as determined by HPLC
A: Poly(ethylene terephthalate)
B: Polysulfone
C: PMMA (PM14)
D: PPMA (PM15)
E: PPMA/PMMA BCP (PM20)

Tab. 2:
Adsorption of protein (human serum albumin) on polymer surfaces

Sample	Polymer	rms[1] [nm]	θ_{adv}; θ_{rec}[2] [°]	γ_{HSA}[3] [mg·m^{-2}]
A	PET-EG3	1.3	74; 70	2.64
B	Polysulfone	2.1	83; 70	2.22
C	PM 14	0.5	79; 60	3.00
D	PM 15	1.0	102; 80	3.27
E	PM 20	0.9	94; 77	3.10

[1] Mean roughness determined by AFM
[2] Advancing (θ_{adv}) and receding (θ_{rec}) contact angle vs. water
[3] Adsorbed amount of HSA

This is also reflected in the protein adsorption. The adsorption of model proteins (human serum albumin, HSA) on PPMA and PMMA homopolymer and BCP films was investigated by the static HPLC technique [20] in order to elucidate the influence of chemical structure and nanostructure on the biological behavior. Thin films with low roughness were again prepared by dip-coating and immersed into a phosphate-buffered solution of 200 ppm HSA. The concentration of adsorbed HSA was measured by HPLC after an incubation time of 60 min (which was shown in preliminary time-dependant measurements to be enough to complete the adsorption process). The results shown in Fig. 11 and Tab. 2 reflect a small influence of the hydrophilicity of PMMA compared to PPMA. Less HSA was adsorbed on the more hydrophilic PMMA. The values were a bit higher than the one for poly(ethylene terephthalate) (PET), a polymer with roughly comparable contact angle and number of hydrophilic ester bonds in the polymer chain, showing that the position of the ester group obviously plays a role. The aromatic polysulfone showed lower HSA adsorption probably due to additional contributions of the $–SO_2$ group. The PPMA/PMMA block copolymers adsorbed an amount of protein intermediate between PPMA and PMMA, thus again reflecting the small difference between the surfaces and the rather not existing influence of the nanostructure on the surface properties.

Applications of nanophase separated PPMA/PMMA diblock copolymers

The applicability of the BCP nanostructures with blocks of different polarity was examined:

- to obtain regular arrays of breath figures after spin coating [21],
- as components in UV-curable epoxies and acrylate resins [22],
- in nanocomposites with layered silicates, and
- in sol-gel reactions to form organic/inorganic hybrids.

In the first step, non-functionalized PPMA/PMMA block copolymers were used. It could be assumed that the different polarity of the blocks (as verified by surface tension measurements) would alter their interaction behavior in the systems. Functionalization reactions according to Fig. 1 provided BCP with functional groups tailored for the above mentioned systems. Allyl-functionalized BCP can be applied as reactive component in UV curing acrylic resins, while OH-terminated PPMA/PMMA block copolymers and triethoxysilane-terminated BCP prepared out of the OH-terminated polymers provide the opportunity for interactions between BCP and

silica (although the different strength of hydrogen bonds between PMMA and silica and PPMA and silica [23] also allows selective interactions between silica and PMMA/PPMA at least in the silica system) which can be used in the mixtures with silica nanoparticles and in sol-gel reactions.
Most of this work was performed in the groups of the EU network. Just one example with results of organic/inorganic hybrids from a sol-gel process obtained together with University of Modena and Reggio Emilia, Italy, is given in the following.
PPMA/PMMA BCP were mixed in a common organic solvent with metal alkoxides to form a silica network with a morphology directed by the nanostructure of the BCP.
Metal alkoxides which were selectively soluble in one phase of the BCP (as obtained by increment calculations) were chosen: OTEOS (octadecyl triethoxysilane) more soluble in PPMA than in PMMA, and TMOS (tetramethoxysilane) more soluble in PMMA than in PMMA.
BCP/metal alkoxide/HCl solutions in THF were used in a dip-coating procedure to yield thin films with the same nanostructure as outlined before (Figs. 7 and 8). These films were subjected to a thermal annealing (2 h at 100 °C) to initiate the silica formation by subsequent hydrolysis / polycondensation of the silanes.
Figure 12 shows that the BCP in mixture with the fast reacting TMOS (10-20 wt% final SiO_2) was also capable to self-organize in some regions of the surface in the concentration range of 10-20 wt% SiO_2. This capability disappeared at higher contents of SiO_2.
Fig. 13 illustrates the possibility that the alkoxysilane (OTEOS) was selectively adsorbed in one phase of the PPMA/PMMA diblock copolymers. The morphology reflects in accordance to former measurements (see Figs. 7 and 8) a mixture of standing and lying PMMA cylinders. The cylinder diameter increased with increasing amount of silica, suggesting that OTEOS adsorbed selectively to the PMMA phase and formed silica around the PMMA cylinders.

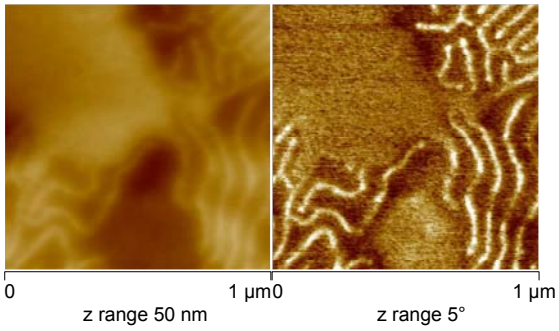

Fig. 12:
AFM image of a thin film containing PM03 and silica (20 wt%) prepared from TMOS by sol-gel reaction in the film

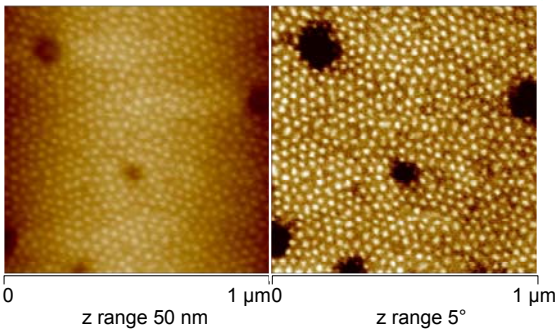

Fig. 13:
AFM image of a thin film containing PM03 and silica (20 wt%) prepared from OTEOS by sol-gel reaction in the film

These sol-gel reactions will be continued with functionalized BCP, including spectroscopic inline-monitoring and direct spectroscopic investigations of the coatings [24].

References

[1] F. S. Bates, G. H. Fredrickson: Ann. Rev. Phys. Chem. 41 (1990), pp. 525-557
[2] F. S. Bates, G. H. Fredrickson: Physics Today 2 (1999), pp. 32-38
[3] M. W. Matsen, F. S. Bates: J. Polym. Sci. B 35 (1997), pp. 945-952
[4] W. A. Lopes, H.M. Jaeger: Nature 414 (2001), pp. 735-738
[5] C. Park, J. Yoon, E. L. Thomas: Polymer 44 (2003), pp. 6725-6760
[6] J. Scherble, B. Stark, B. Stühn, J. Kressler, H. Budde, S. Höring, W. Schubert, P. Simon, M. Stamm: Macromolecules 32 (1999), pp. 1859-1864
[7] R. Keska, D. Pospiech, K. Eckstein, D. Jehnichen, S. Ptacek, L. Häußler, P. Friedel, A. Janke, B. Voit: J. Nanostr. Polym. Nanocomp. 2 (2006), pp. 43-52
[8] R. D. Allen, T. E. Long, J. E. McGrath: Polym. Bull. 15 (1986), pp. 127-134
[9] E. T. B. Al-Takrity, A. D. Jenkins, D. R. M. Walton: Makromol. Chem. 191 (1990), pp. 3077-3080
[10] B. C. Anderson, G. D. Andrews, P. Arthur, H. W. Jacobson, L. R. Melby, A. J. Playtis, W. H. Sharkey: Macromolecules 14 (1981), pp. 1601-1603
[11] M. Laurenti: Master of Science Thesis, University of Perugia, Italy (2007)
[12] L. Leibler: Macromolecules 13 (1980), pp. 1602-1617
[13] H. Benoit, H. Hadziioannou: Macromolecules 21 (1988), pp. 1449-1464
[14] A. John, P. Friedel, R. Netz, D. Pospiech, D. Jehnichen, A. Gottwald: Macromol. Theory Simul. (2004), pp. 702-710
[15] D. Pospiech, A. Gottwald, D. Jehnichen, P. Friedel, A. John, C. Harnisch, D. Voigt, G. Khimich, A. Y. Bilibin: Colloid Polym. Sci. 280 (2002), pp. 1027-1037
[16] D. Jehnichen, D. Pospiech, P. Friedel, R. Keska, J. Müller, A. Korwitz, S. Ptacek, S. Funari, M. Dommach: Phase behavior of weakly phase separated PPMA-PMMA diblock copolymers.– HASYLAB Annual Report (2006), Hamburg, http://hasylab.desy.de
[17] P. Müller-Buschbaum: Anal. Bioanal. Chem. 376 (2003), pp. 3-10
[18] P. Busch: Lamellare Orientierung in dünnen Diblockcopolymerfilmen – Strukturen an der Filmoberfläche und im Filminneren.– PhD Thesis, Universität Leipzig (2003)
[19] R. Keska: Study of the phase behavior of poly(n-alkyl methacrylate-*b*-methyl methacrylate) diblock copolymers and its influence on the wettability of polymer surfaces.– PhD Thesis, Technische Universität Dresden (2006)
[20] T. Klose, P. B. Welzel, C. Werner: Coll. Surf. 51 (2006), pp. 1-9
[21] F. Pilati, M. Montecchi, P. Fabbri, A. Synytska, M. Messori, M. Toselli, K. Grundke, D. Pospiech: J. Coll. Surf. Sci. 315 (2007), pp. 210-222
[22] M. Sangermano, B. Voit, E. Amerio, A. Di Gianni, A. Priola, D. Pospiech: Macromol. Symp. 254 (2007), pp. 9-15
[23] A. Sargsyan: Quantification of the immobilized fraction in polymer inorganic nanocomposites.– PhD Thesis, Universität Rostock (2007)
[24] D. Fischer, D. Pospiech, U. Scheler, R. Navarro, M. Messori, P. Fabbri: Monitoring of the sol-gel synthesis of organic-inorganic hybrids by ATR/IR-, NIR- and Raman spectroscopy.– Macromol. Symp., in print